

Content-based medical image retrieval method using multiple pre-trained convolutional neural networks feature extraction models



Ahmad A. Alzahrani ¹, Ali Ahmed ^{2,*}, Alisha Raza ³

¹Faculty of Computing and Information Technology, King Abdulaziz University, Jeddah, Saudi Arabia

²Faculty of Computing and Information Technology, King Abdulaziz University–Rabigh, Rabigh, Saudi Arabia

³Department of Computer Science, Maulana Azad National Urdu University, Hyderabad, India

ARTICLE INFO

Article history:

Received 16 January 2024

Received in revised form

2 June 2024

Accepted 8 June 2024

Keywords:

Image retrieval

Content-based medical image retrieval

Feature extraction

Pre-trained deep CNNs

ABSTRACT

Content-based medical image retrieval (CBMIR), a specialized area within content-based image retrieval (CBIR), involves two main stages: feature extraction and retrieval ranking. The feature extraction stage is particularly crucial for developing an effective retrieval system with high performance. Lately, pre-trained deep convolutional neural networks (CNNs) have become the preferred tools for feature extraction due to their excellent performance and versatility, which includes the ability to be re-trained and adapt through transfer learning. Various pre-trained deep CNN models are employed as feature extraction tools in CBMIR systems. Researchers have effectively used many such models either individually or in combined forms by merging feature vectors from several models. In this study, a method using multiple pre-trained deep CNNs for CBMIR is introduced, utilizing two popular models, ResNet-18 and GoogleNet, for extracting features. This method combines the feature vectors from both models in a way that selects the best model for each image based on the highest classification probability during training. The method's effectiveness is assessed using two well-known medical image datasets, Kvasir and PH². The evaluation results show that the proposed method achieved average precision scores of 94.13% for Kvasir and 55.67% for PH² at the top 10 cut-offs, surpassing some leading methods in this research area.

© 2024 The Authors. Published by IASE. This is an open access article under the CC BY-NC-ND license (<http://creativecommons.org/licenses/by-nc-nd/4.0/>).

1. Introduction


Feature extraction is considered an important stage in any content-based image retrieval (CBIR) method; different approaches for deep learning and pre-trained methods are used for this purpose. The retrieval and classification of lung illnesses based on lung X-ray images in order to enable early diagnosis has been successfully implemented in the literature. In a previous survey (Bharati et al., 2020), they covered a content-based medical image retrieval (CBMIR) system that is based on the ability of neural networks with deep layers to identify and classify disease-specific features through the use of transfer learning techniques. Bharati et al. (2020) also extended their study to different deep-learning algorithms, which would increase the performance

of the system and also be used in real-world applications. Using pre-trained deep convolutional neural networks (CNNs) combined with a sparse features extraction model has shown good performance, as in Sezavar et al. (2019). In their study, they used deep CNNs and a sparse model and extracted the deep features of the image dataset; in the end, their model improved the retrieval accuracy. A novel hybrid deep learning and machine learning-based CBIR system that uses a transfer learning technique was successfully implemented in (Sikandar et al., 2023). The authors of the study introduced an innovative combination of deep learning and machine learning approaches and employed transfer learning to extract features based on ResNet-18 and VGG16 pre-trained models and the KNN algorithm. Their achievement was improved by up to 100%, and they extended their model for use in many applications that need CBIR, such as digital libraries, historical research, fingerprint identification, and crime prevention. A recent intensive review study of deep learning-based development models for CBIR can be found in Dubey (2021). In their survey, the taxonomy used covered

* Corresponding Author.

Email Address: aabdelrahim@kau.edu.sa (A. Ahmed)

<https://doi.org/10.21833/ijaas.2024.06.019>

 Corresponding author's ORCID profile:

<https://orcid.org/0000-0002-8944-8922>

2313-626X/© 2024 The Authors. Published by IASE.

This is an open access article under the CC BY-NC-ND license

(<http://creativecommons.org/licenses/by-nc-nd/4.0/>)

different supervision, different networks, different descriptor types, and different retrieval types. The survey presented in their study will help to develop further research in image retrieval using deep learning; more related and recent surveys are also found in [Latif et al. \(2019\)](#), [Fu et al. \(2020\)](#), and [Garg and Dhiman \(2021\)](#). These studies utilized the power and effectiveness of pre-trained deep CNNs to develop multiple convolutional retrieval methods based on the maximum classification probability for CBMIR. The main contribution of the paper is summarized as follows:

- Extract effective image feature descriptors based on the maximum probability of either ResNet-18 or GoogleNet pre-trained models for both image collection and unknown class label query images.
- Develop an effective retrieval method for CBMIR based on the above efficient representative feature descriptors.
- Enhance the retrieval performance of CBMIR using the above efficient features extracted based on most of the well-known pre-trained deep CNNs models.

The rest of this paper is organized as follows: Section 2 reviews previous studies and related work. Section 3 explains the basic concepts and ideas behind the proposed retrieval methods. Section 4 presents the experimental results and discussion. Finally, Section 5 provides the conclusion and suggestions for future research.

2. Related works

Multichannel deep CNNs were successfully used for multilane traffic speed prediction; the power of deep CNNs was utilized and extended for use in an effective manner to learn the features and correlations between individual lanes ([Ke et al., 2020](#)). Also, multiple deep CNNs were implemented for large-scale video classification and achieved acceptable accuracy results ([Karpathy et al., 2014](#)). In their study, they showed that the fusion process required when using multiple deep CNNs could be performed either in the early stages by modifying the first layers of convolutional filters and adjusting the input layers accordingly or later by placing two separate single-frame networks. When using multiple deep CNNs, the combination process could be performed in different ways, as in [Sezavar et al. \(2019\)](#); in their studies, they extracted image features via a combination of CNNs and sparse representation. They took advantage of the high accuracy of deep CNNs and reasonable speed by using a sparse model. This sparse approach focuses only on a subset of important features instead of all image features. The tendency for correctly classified images to have higher probabilities was effectively investigated for solving classification problems in various tasks, including computer vision, natural language processing, and automatic speech recognition ([Hendrycks and Gimpel, 2016](#)). Recently,

multiple pre-trained CNNs have been used for CBIR by combining and fusing the features of different images using an enhanced optimization algorithm. In their recent studies, deep feature extraction was performed by utilizing three deep learning models: VGG-16, Inception v3, and Xception ([Raju et al., 2022](#)). The feature matrix of medical images could be extracted from fully connected layers of pre-trained deep CNNs, which were divided into branches, and then separate feature extraction was done for each branch; finally, multiple features flattened were obtained for a single vector ([Alappat et al., 2021](#)). Some of the well-known pre-trained deep CNNs were successfully used to develop effective retrieval performance methods for CBMIR ([Ahmed, 2021](#); [Ahmed and Mohamed, 2021](#); [Ahmed, 2022](#); [Ahmed et al., 2022](#)).

3. Methodology

The general framework of the CBMIR system is shown in [Fig. 1](#). As standard, any image retrieval process begins with collecting the specific medical images used for that purpose, followed by the process of pre-processing images. In this research, well-known Kvasir medical images used for gastrointestinal disease detection were used as the main image dataset, which was used in a number of previous and recent studies. This is shown in the next section, which gives more detail about these medical image datasets. No pre-processing operations were applied in this study, except the process of standardizing the input image sizes when entered into the deep learning model to generate digital features. The next step in the main framework is to pass these images to the multiple pre-trained deep convolution neural network (MPCNN) feature extraction stage proposed in this study, as shown by the red dashed line in [Fig. 1](#).

After generating the numeric features, the similarity calculation stage is performed, in which the similarity between an image query posted by the user and all of the images in the image database is calculated using one of the well-known similarity coefficients. This study uses the Euclidean distance standard similarity measure, which is the most widely used in retrieval processes in general and image retrieval operations in particular. Finally, the sorting and retrieval stage is performed, in which the retrieved images are arranged in descending order, placing images with the highest similarity at the top. In this final stage, the retrieval model retrieves images that are most similar to the user query. The process of MPCNN feature extraction, shown by the dashed line, represents the proposed contributions in this study; this process is explained in detail in the current section. The proposed multiple pre-trained deep convolution neural networks MPCNNsRM, as shown in the general framework by a dashed line, is elaborated in [Fig. 2](#). Similar to most CBMIR systems, this proposed method is divided into two parts or phases: the offline phase and the online phase. The first phase is executed only once for the image

database or with the addition of new medical images, while the second phase is carried out with every process of querying the retrieval system by the user.

All of the remaining computational processes are only based on the numerical features that were generated.

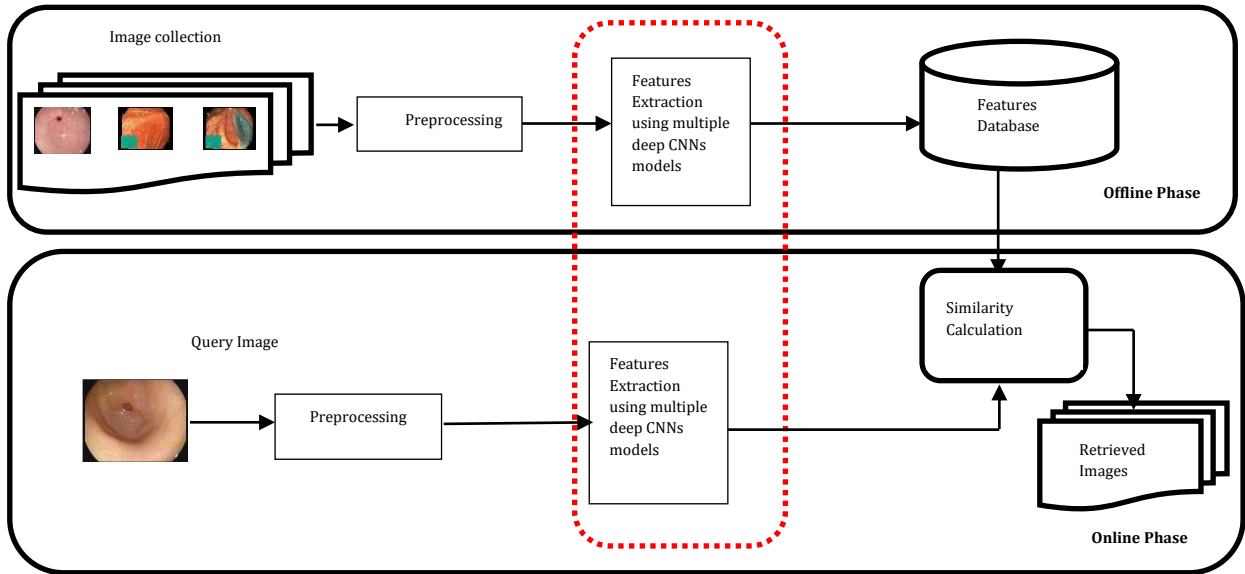


Fig. 1: Workflow of the CBMIR method with our proposed multiple deep CNNs models

During the offline phase, all collected training images were used for feature extraction using well-known pre-trained deep CNNs, ResNet-18, and GoogleNet. These pre-trained models were adapted for feature extraction by retraining the high-level layers while using the weights from the low-level layers, leveraging transfer learning concepts. All medical images were input with class labels during this phase. The maximum classification probability for all images was estimated by the two selected pre-trained CNNs, and their feature vectors were used as feature representatives for the entire dataset. The

same method was applied to extract feature vectors from query images, but instead of using class labels, an auto-encoder was used. After calculating similarity, retrieval performance was measured in terms of recall and precision for the top ten retrieved images. The following two algorithms describe the proposed method. For each image query, the maximum classification probability from the two pre-trained CNNs was selected, and the feature vector was used as the feature representative for the query image.

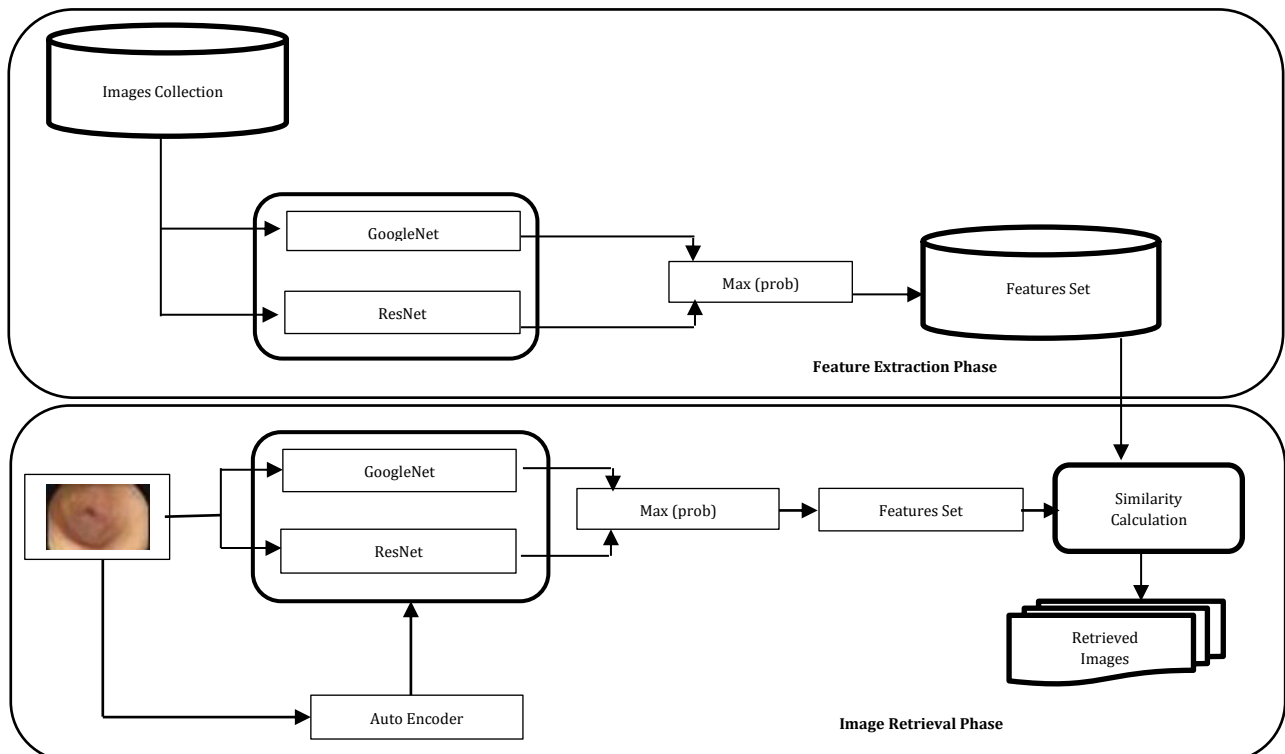


Fig. 2: Proposed multiple deep convolution neural networks model for medical feature extraction and retrieval

Algorithm 1: Feature extraction phase algorithm

Input: image collection for all classes
 Output: feature vector for testing images
 1: Start
 2: Split image collection into (0.6) training (m) and (0.4) testing (n)
 2: For i = 1: m // number of images in training collection
 3: re-train ResNet-18 and GoogleNet based on image classes
 4: End // for1
 5: For i = 1: n // number of images in test collection
 6: compute classification label and classifier prob for ResNet-18 and GoogleNet
 7: if ResNet-18 Prob > GoogleNet Prob
 8: ResNet-18_Features = Feature vector extracted using ResNet-18
 9: else
 10: Google_Features = Feature vector extracted using Google
 11: End
 12: Image_Features=[ResNet-18_Features; Google_Features]
 13: End // Start

Algorithm 2: Image Retrieval Phase Algorithm

Input: medical image from unknown classes
 Output: top relevant images
 1: Start
 2: Read an image as query image
 3: generate the auto encoder for an image and used it as a class label
 4: compute classification label and classifier prob using ResNet-18 and GoogleNet for query image
 5: if ResNet-18 Prob > GoogleNet Prob
 6: Query_Features = Feature vector extracted using ResNet-18

7: else
 8: Query_Features = Feature vector extracted using Google
 9: Calculate the similarity measure between query feature vector and all images features
 10: Calculate top retrieved top images and calculate an average recall and precision
 11: End if
 12: End // start

3.1. Medical image dataset

Datasets of Kvasir images (Pogorelov et al., 2017) and PH² images (Mendonça et al., 2013), two of the most popular medical image databases, were used in this study's experiments. The updated Kvasir software includes 4,000 colored endoscopic images with professional annotations. Based on medical perception and concern, these 500 images in each of the eight classes that make up this dataset were grouped together. A collection of 200 dermoscopic images separated into three classifications makes up the second dataset, which is intended for research and benchmarking. Samples of these two medical images are shown in Fig. 3; these two datasets were used in previous studies (Ahmed, 2020; Ahmed and Malebary, 2020; Ahmed et al., 2023). After the successful implementation of our proposed method, the results of effective retrieval performance will help in the area of gastrointestinal image indexing and retrieval, thus facilitating the process of case-based learning and diagnosis-based methods.

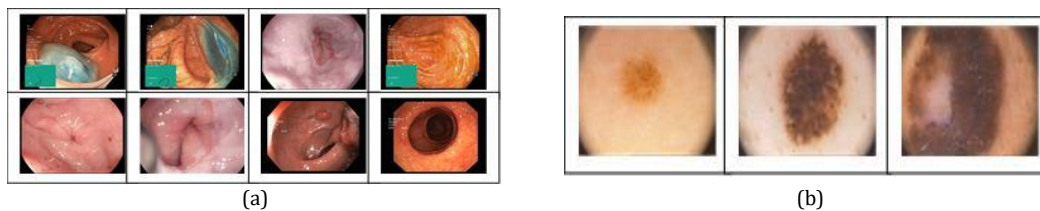


Fig. 3: Image sample for (a) Kvasir dataset and (b) PH² dataset

3.2. Evaluation measures

Two evaluation measures were used in this study, as in many related studies: recall and precision. Both of these measures were calculated using the top 10 and top 20 relevant retrieved images. The following two evaluation measures can be explained as follows:

$$\text{precision} = \frac{\text{number of relevant images retrieved}}{\text{total number of retrieved images}}$$

$$\text{recall} = \frac{\text{number of relevant images retrieved}}{\text{total number of relevant images}}$$

4. Experimental results and discussion

As shown in the general diagram for medical image retrieval, as well as in the diagram for merging two trained network models for CBMIR, as given in Figs. 1 and 2, the retrieval process generally takes place in two stages. The first stage is that in which all medical images are used for the purpose of extracting numeric features, while the second stage is very important, as the accuracy of the retrieval is

based and calculated upon this. At this stage, a number of images from each class could be selected as an image query, and then the retrieval performance could be calculated. Here, recall and precision are used as the main performance measures, and all of our results are computed at a cut-off top 10 and top 20. This will be explained in the following paragraphs.

In this study, the main experiment was performed to evaluate and prove the best retrieval method based on MPCNN image features. To reach this goal, three different results were reported: two retrieval results based on ResNet-18 and GoogleNet features individually and the third result based on our proposed multiple deep CNN features. For all three types of experiments, five images were selected randomly from each image class for both datasets. Average precisions for each class, as well as for all classes, are presented in Table 1 and Table 2 for the Kvasir and PH² datasets (for both the top 10 and top 20), respectively. The first observation of Table 1 for Kvasir images shows that the average precisions are 94.13% and 91.38% for both cut-off

top retrievals, which outperformed each of the ResNet-18 and GoogleNet models. Also, all average precisions for the eight classes in a combined method for the top 10 are superior to all average values in GoogleNet and all seven classes in ResNet-18, except for the first DLP class, where ResNet-18 showed the best results. A similar observation could be seen for the top 20 results, in which the combined method showed the best performance. The best retrieval performance could also be observed from Table 2 for PH² images, in which the combined method has the highest average precision while ResNet-18 and GoogleNet have similar results for both the top 10 and top 20 cut-off values.

Precisions and recalls at different cut-off values were compared for the three retrieval methods and two datasets; the results are presented in Figs. 4a and 4b. The upper behavior of the lines shows the combined method for recall; precision plotting indicates the best retrieval performance for the proposed retrieval method, while ResNet-18 was better than GoogleNet. Similar observations could be noted from Figs. 5a and 5b, which show numbers of retrieved images at different cut-off precision values.

Table 1: Precision at top 10 and top 20 for Kvasir Images

	ResNet	GoogleNet	MPCNNsRM
10			
DLP	0.9500	0.8200	0.9400
DRM	0.8300	0.8800	0.9300
Esophagitis	0.6300	0.6700	0.8500
Normal caecum	0.9800	0.9800	1.0000
Normal pylorus	0.9300	0.9500	0.9800
Normal z line	0.7100	0.8000	0.8800
Polyps	0.9800	0.9200	1.0000
Ulcerative colitis	0.9000	0.8600	0.9500
Average	0.8638	0.8600	0.9413
20			
DLP	0.8150	0.8450	0.9100
DRM	0.8400	0.8550	0.9100
Esophagitis	0.6600	0.6700	0.7100
Normal caecum	0.9900	0.9200	0.9900
Normal pylorus	0.9450	0.9100	0.9850
Normal z line	0.7950	0.7100	0.8950
Polyps	0.9200	0.9850	0.9900
Ulcerative colitis	0.8300	0.8300	0.9200
Average	0.8543	0.8400	0.9138

Table 2: Precision at top 10 and top 20 for PH² Images

	ResNet	GoogleNet	MPCNNsRM
10			
Normal	0.3800	0.3800	0.4900
Atypical nevus	0.3800	0.4200	0.5300
Melanoma	0.5700	0.5000	0.6500
Average	0.4433	0.4333	0.5567
20			
Normal	0.4200	0.4200	0.4400
Atypical nevus	0.3900	0.3900	0.5100
Melanoma	0.4300	0.4400	0.6100
Average	0.4133	0.4167	0.5200

More analysis of the results was performed using the Kendall W concordance test (Sidney, 1957) and upper and lower bounds of confidence intervals. The Kendall W test is widely used for comparing and ranking a group of retrieval methods or coefficients; it has been used in many studies to compare information and CBIR retrieval methods (Ahmed et al., 2014; Yang et al., 2020; Voorhees et al., 2022). In this study and many similar retrieval performance

evaluations and rankings, the inputs for this significant test are the average precision values per class, while the outputs of the test are the Kendall coefficient (W) and the associated level of ranking or significance (P). After performing this test for both datasets, the results are presented in Table 3, in which the ranking order of the combined method has the best performance at the related confidence (W) percentage values. The other analytical results of the precision performance bound are shown in Figs. 6a and 6b for both datasets.

Table 3: Ranking of different retrieval methods for three retrieval methods using Kendall w test of precision values for two data sets (at top 10 and 20)

Dataset	W	P	Ranking
Top 10			
Kvasir	59.3	0.090	MPCNNsRM > GoogleNet > ResNet
PH ²	81.5	0.086	MPCNNsRM > ResNet > GoogleNet
Top 20			
Kvasir	70.4	0.060	MPCNNsRM > GoogleNet > ResNet
PH ²	93.3	0.061	MPCNNsRM > GoogleNet > ResNet

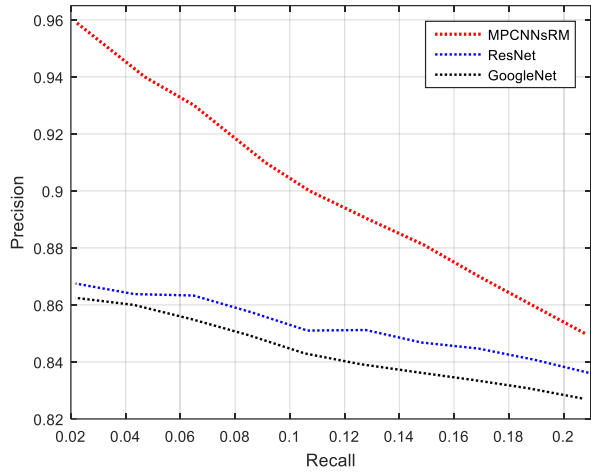
For the comparison purposes, our findings and retrieval results in this study are compared with six similar methods: CBGIR-GPD (Hu et al., 2021), MIRS (Kasban and Salama, 2019), OCAM (Öztürk et al., 2023), SIFT-mLBP (Satish and Supreethi, 2017), VLAD (Spyromitros-Xioufis et al., 2014) and RFRM (Ahmed, 2020), as shown in Table 4. The first method implemented a modified version of ResNet-18 for generating binary hash codes for Kvasir, while the second method used wavelet optimization and adaptive block truncation coding. The third approach used an opponent class adaptive margin loss method, while the fourth utilized the relevance feedback Bayesian network after the SIFT-modified LBP descriptor for multi-modal medical images. The fifth method implemented quantification in large-scale image retrieval, while the last comparison-based method applied a relevance feedback retrieval method based on voting processes. Finally, visual results for the three retrieval methods are shown in Fig. 7 and Fig. 8, which illustrate a sample of the top retrieved images for some classes of two datasets.

Table 4: Image retrieval performance compared with different retrieval approaches

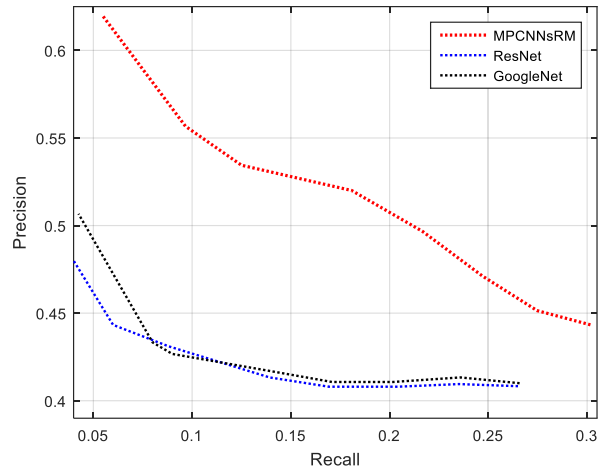
Method	Dataset	Precision @P10	Precision @P20
CBGIR-GPD	Kvasir	0.9270±0.006	-
MIRS	Kvasir	0.6120	0.5980
MIRS	VIA -ELCAP CT	0.9390	0.9140
OCAM	Kvasir	0.9075	0.8897
SIFT-mLBP	Mammogram	0.8800	-
VLAD	Multi-modal	-	0.9061 ±0.00459
RFRM	Kvasir	0.8500	0.8625
MPCNNsRM (Ours)	Kvasir	0.9413	0.9138

5. Conclusion

In this study, a multiple pre-trained deep convolution neural networks-based retrieval method (MPCNNsRM) for CBMIR was proposed and developed.

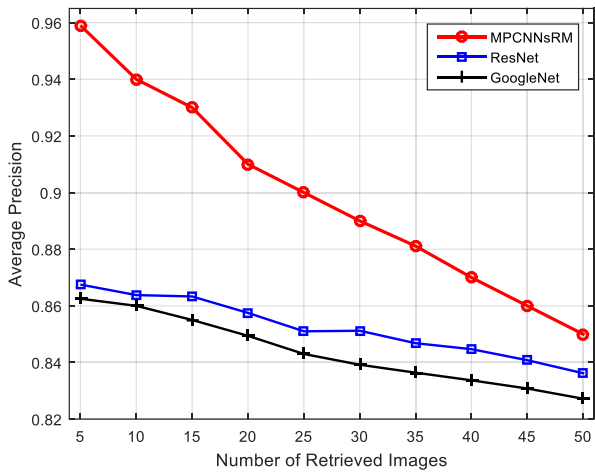


(a) Kvasir images

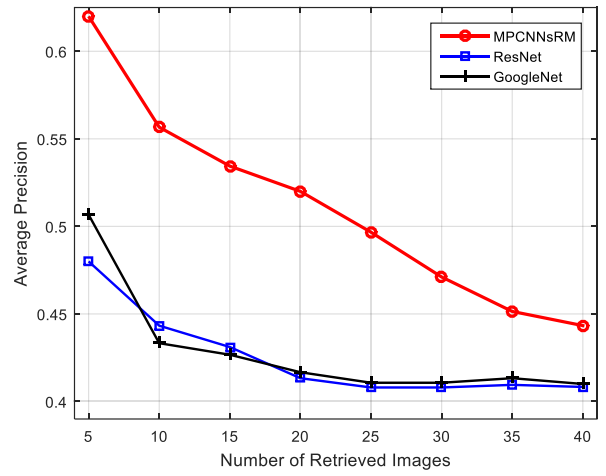


(b) PH² images

Fig. 4: Recall and precision

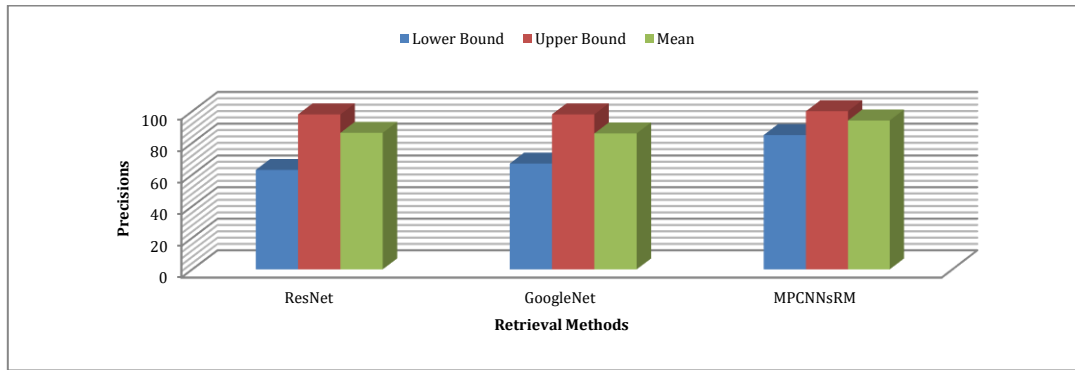


(a) Kvasir images

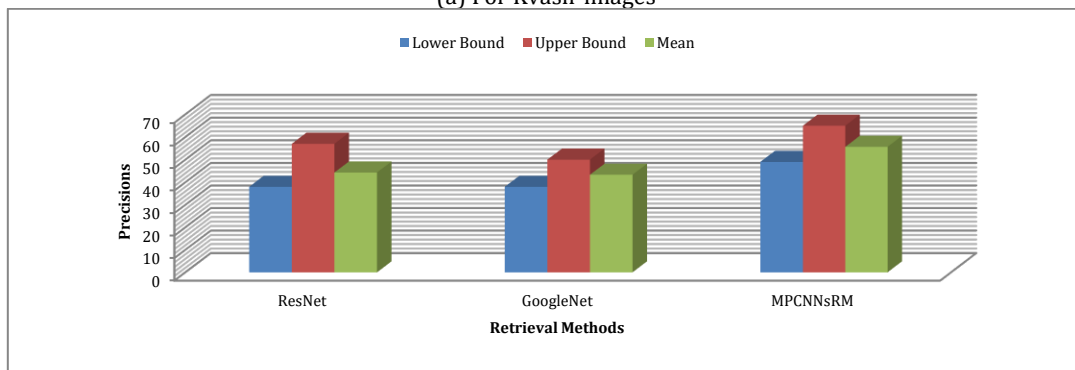


(b) PH² images

Fig. 5: Average precision at different top



(a) For Kvasir images



(b) For PH² images

Fig. 6: Precisions performance bounds

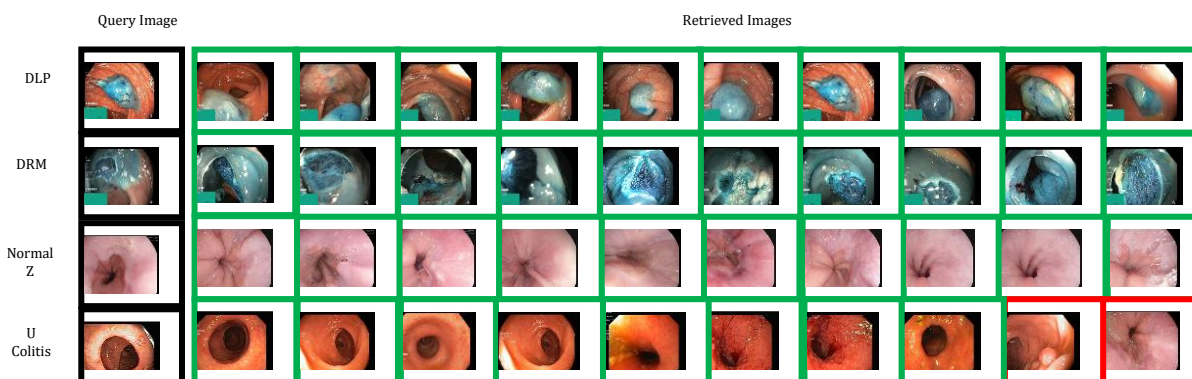


Fig. 7: Sample images retrieved for some classes of Kvasir images using MPCNNsRM (Red frames show false retrieved images)

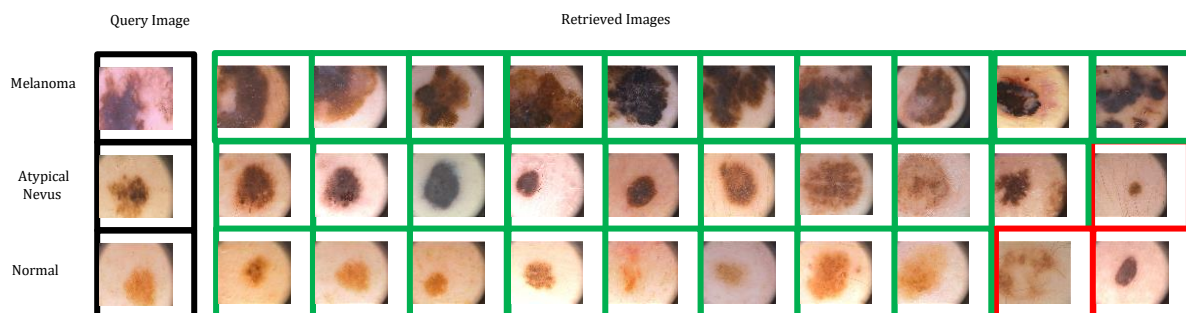


Fig. 8: Sample images retrieved for all classes of PH² images using MPCNNsRM (Red frames show false retrieved images)

After using these well-known pre-trained deep CNN models, two main benefits were achieved. First, the high-performance capabilities of recent deep learning models were utilized. Second, combining feature extractions from multiple models improved retrieval performance. This combination created informative and accurate image features. The retrieval performance, measured by recall and precision, surpassed some of the most well-known methods in this field, as shown in the comparison table. Additionally, our method is simple and cost-effective because it uses existing high-performance deep learning models. For future work, more than one pre-trained deep CNN model can be used for feature extraction. Simple fusion methods or classification probabilities based on weight and voting approaches could be employed to combine the image feature vectors.

Acknowledgment

This research work was funded by the Institutional Fund Project under grant no. (IFPIP:1173-611-1443). The authors gratefully acknowledge the technical and financial support provided by the Ministry of Education and King Abdulaziz University, DSR, Jeddah, Saudi Arabia.

Compliance with ethical standards

Conflict of interest

The author(s) declared no potential conflicts of interest with respect to the research, authorship, and/or publication of this article.

References

- Ahmed A (2020). Implementing relevance feedback for content-based medical image retrieval. *IEEE Access*, 8: 79969-79976. <https://doi.org/10.1109/ACCESS.2020.2990557>
- Ahmed A (2021). Pre-trained CNNs models for content based image retrieval. *International Journal of Advanced Computer Science and Applications*, 12(7): 200-206. <https://doi.org/10.14569/IJACSA.2021.0120723>
- Ahmed A (2022). Classification of gastrointestinal images based on transfer learning and denoising convolutional neural networks. In the *Proceedings of International Conference on Data Science and Applications*, Springer Singapore, Kolkata, India, 1: 631-639. https://doi.org/10.1007/978-981-16-5120-5_48
- Ahmed A and Malebary SJ (2020). Query expansion based on top-ranked images for content-based medical image retrieval. *IEEE Access*, 8: 194541-194550. <https://doi.org/10.1109/ACCESS.2020.3033504>
- Ahmed A and Mohamed S (2021). Implementation of early and late fusion methods for content-based image retrieval. *International Journal of Advanced and Applied Sciences*, 8(7): 97-105. <https://doi.org/10.21833/ijaas.2021.07.012>
- Ahmed A, Almagrabi AO, and Barukab OM (2023). A content-based medical image retrieval method using relative difference-based similarity measure. *Intelligent Automation and Soft Computing*, 37(2): 2355-2370. <https://doi.org/10.32604/iasc.2023.039847>
- Ahmed A, Almagrabi AO, and Osman AH (2022). Pre-trained convolution neural networks models for content-based medical image retrieval. *International Journal of Advanced and Applied Sciences*, 9(12): 11-24. <https://doi.org/10.21833/ijaas.2022.12.002>
- Ahmed A, Saeed F, Salim N, and Abdo A (2014). Condorcet and borda count fusion method for ligand-based virtual screening. *Journal of Cheminformatics*, 6: 19. <https://doi.org/10.1186/1758-2946-6-19>
PMid:24883114 PMCID:PMC4026830

- Alappat AL, Nakhate P, Suman S, Chandurkar A, Pimpalkhute V, and Jain T (2021). CBIR using pre-trained neural networks. Arxiv Preprint Arxiv:2110.14455. <https://doi.org/10.48550/arXiv.2110.14455>
- Bharati S, Podder P, and Mondal MRH (2020). Hybrid deep learning for detecting lung diseases from X-ray images. Informatics in Medicine Unlocked, 20: 100391. <https://doi.org/10.1016/j.imu.2020.100391> **PMid:32835077 PMCID:PMC7341954**
- Dubey SR (2021). A decade survey of content based image retrieval using deep learning. IEEE Transactions on Circuits and Systems for Video Technology, 32(5): 2687-2704. <https://doi.org/10.1109/TCSVT.2021.3080920>
- Fu Y, Lei Y, Wang T, Curran WJ, Liu T, and Yang X (2020). Deep learning in medical image registration: A review. Physics in Medicine and Biology, 65(20): 20TR01. <https://doi.org/10.1088/1361-6560/ab843e> **PMid:32217829 PMCID:PMC7759388**
- Garg M and Dhiman G (2021). A novel content-based image retrieval approach for classification using GLCM features and texture fused LBP variants. Neural Computing and Applications, 33(4): 1311-1328. <https://doi.org/10.1007/s00521-020-05017-z>
- Hendrycks D and Gimpel K (2016). A baseline for detecting misclassified and out-of-distribution examples in neural networks. Arxiv Preprint Arxiv:1610.02136. <https://doi.org/10.48550/arXiv.1610.02136>
- Hu H, Zheng W, Zhang X, Zhang X, Liu J, Hu W, Duan H, and Si J (2021). Content-based gastric image retrieval using convolutional neural networks. International Journal of Imaging Systems and Technology, 31(1): 439-449. <https://doi.org/10.1002/ima.22470>
- Karpathy A, Toderici G, Shetty S, Leung T, Sukthankar R, and Fei-Fei L (2014). Large-scale video classification with convolutional neural networks. In the Proceedings of the IEEE Conference on Computer Vision and Pattern Recognition, Computer Vision Foundation, Columbus, USA: 1725-1732. <https://doi.org/10.1109/CVPR.2014.223>
- Kasban H and Salama DH (2019). A robust medical image retrieval system based on wavelet optimization and adaptive block truncation coding. Multimedia Tools and Applications, 78(24): 35211-35236. <https://doi.org/10.1007/s11042-019-08100-3>
- Ke R, Li W, Cui Z, and Wang Y (2020). Two-stream multi-channel convolutional neural network for multi-lane traffic speed prediction considering traffic volume impact. Transportation Research Record, 2674(4): 459-470. <https://doi.org/10.1177/0361198120911052>
- Latif A, Rasheed A, Sajid U, Ahmed J, Ali N, Ratyal NI, Zafar B, Dar SH, Sajid M, and Khalil T (2019). Content-based image retrieval and feature extraction: a comprehensive review. Mathematical Problems in Engineering, 2019: 9658350. <https://doi.org/10.1155/2019/9658350>
- Mendonça T, Ferreira PM, Marques JS, Marcal AR, and Rozeira J (2013). PH²-A dermoscopic image database for research and benchmarking. In the 35th Annual International Conference of the IEEE Engineering in Medicine and Biology Society, IEEE, Osaka, Japan: 5437-5440. <https://doi.org/10.1109/EMBC.2013.6610779> **PMid:24110966**
- Öztürk Ş, Çelik E, and Çukur T (2023). Content-based medical image retrieval with opponent class adaptive margin loss. Information Sciences, 637: 118938. <https://doi.org/10.1016/j.ins.2023.118938>
- Pogorelov K, Randel KR, Griwodz C, Eskeland SL, de Lange T, Johansen D, Spampinato C, Dang-Nguyen DT, Lux M, Schmidt PT, and Halvorsen P (2017). Kvasir: A multi-class image dataset for computer aided gastrointestinal disease detection. In the Proceedings of the 8th ACM on Multimedia Systems Conference, ACM, Taipei, Taiwan: 164-169. <https://doi.org/10.1145/3083187.3083212>
- Raju GK, Padmanabham P, and Govardhan A (2022). Enhanced content-based image retrieval with trio-deep feature extractors with multi-similarity function. International Journal of Intelligent Engineering and Systems, 15(6): 511-525. <https://doi.org/10.22266/ijies2022.1231.46>
- Satish B and Supreethi KP (2017). Content based medical image retrieval using relevance feedback Bayesian network. In the International Conference on Electrical, Electronics, Communication, Computer, and Optimization Techniques, IEEE, Mysuru, India: 424-430. <https://doi.org/10.1109/ICEECCOT.2017.8284542>
- Sezavar A, Farsi H, and Mohamadzadeh S (2019). Content-based image retrieval by combining convolutional neural networks and sparse representation. Multimedia Tools and Applications, 78: 20895-20912. <https://doi.org/10.1007/s11042-019-7321-1>
- Sidney S (1957). Nonparametric statistics for the behavioral sciences. The Journal of Nervous and Mental Disease, 125(3): 497. <https://doi.org/10.1097/00005053-195707000-00032>
- Sikandar S, Mahum R, and Alsaman A (2023). A novel hybrid approach for a content-based image retrieval using feature fusion. Applied Sciences, 13(7): 4581. <https://doi.org/10.3390/app13074581>
- Spyromitros-Xioufis E, Papadopoulos S, Kompatsiaris IY, Tsoumakas G, and Vlahavas I (2014). A comprehensive study over VLAD and product quantization in large-scale image retrieval. IEEE Transactions on Multimedia, 16(6): 1713-1728. <https://doi.org/10.1109/TMM.2014.2329648>
- Voorhees EM, Soboroff I, and Lin J (2022). Can old TREC collections reliably evaluate modern neural retrieval models? Arxiv Preprint Arxiv:2201.11086. <https://doi.org/10.48550/arXiv.2201.11086>
- Yang S, Zhang Y, Shen J, Dai Y, Ling Y, Lu H, Zhang R, Ding X, Qi H, Shi Y, and Zhang Z (2020). Clinical potential of UTE-MRI for assessing COVID-19: Patient-and lesion-based comparative analysis. Journal of Magnetic Resonance Imaging, 52(2): 397-406. <https://doi.org/10.1002/jmri.27208> **PMid:32491257 PMCID:PMC7300684**